JCB

Graham et al., https://doi.org/10.1083/jcb.201706097

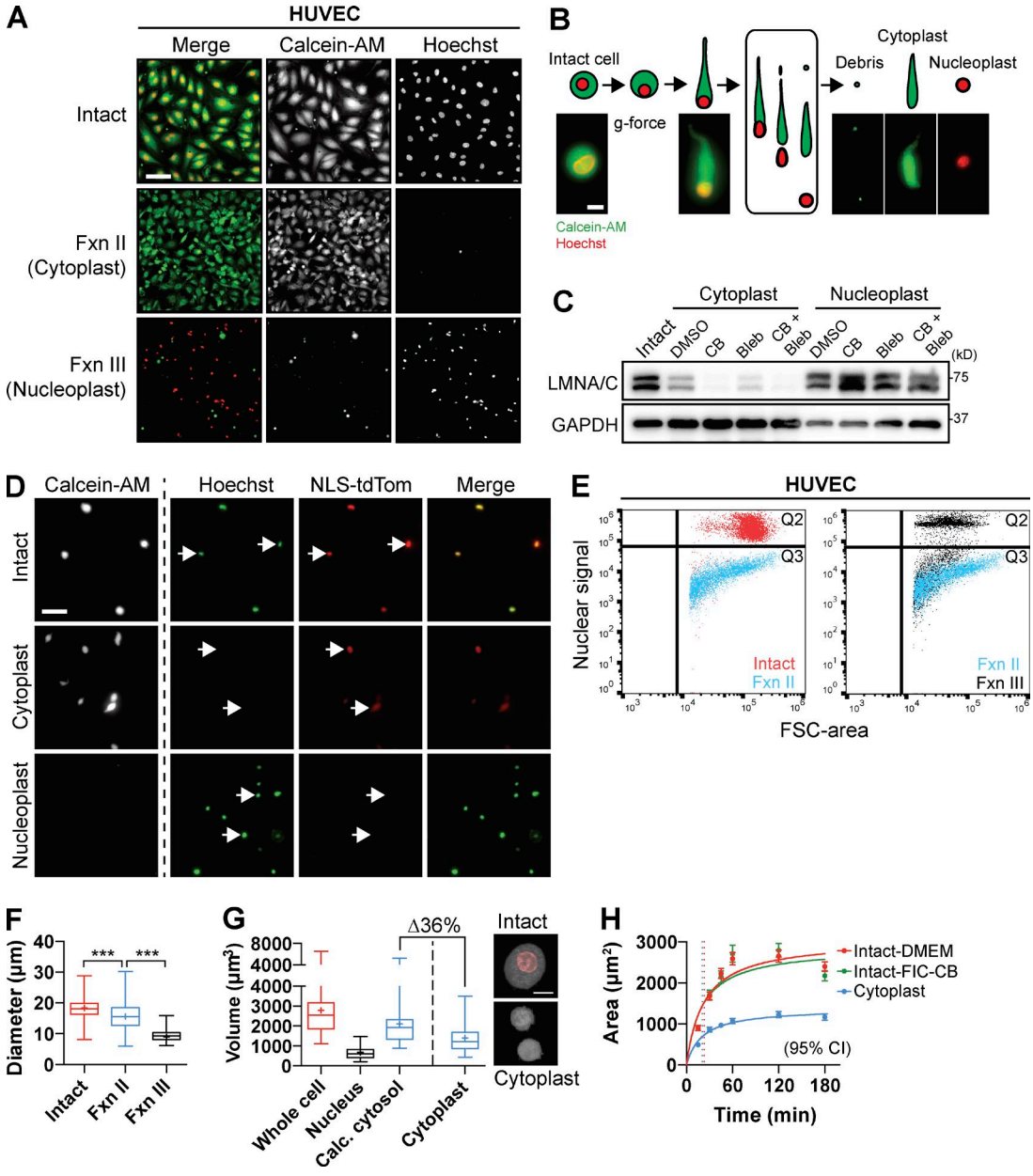

Figure S1. **Characterization of enucleation and cytoplasts. (A)** Fluorescence images of HUVEC intact cells and fractions (Fxn) 2 h after enucleation. Bar, 50 µm. **(B)** Illustration and evidence that enucleation occurs through continuous repositioning of the nucleus through the cell. Bar, 10 µm. **(C)** Western blots showing nuclear content (LMNA/C) from cytoplast and nucleoplast fractions of REF52 fibroblasts enucleated with cytochalasin (CB) and/or blebbistatin (bleb). **(D)** Images immediately after enucleation of stable REF52-NLS-tdTomato line showing tdTomato signal in cytoplasts with loss in nucleoplasts. Arrows point to examples from populations. Bar, 50 µm. **(E)** Cytometric profiles of stained HUVEC populations with a fluorescent nuclear dye (Vybrant DyeCycle Green). Q2 is region containing positive nuclear staining. Q3 is negative for nuclear staining. FSC, forward scatter. **(F)** Cell diameter measurements of REF52 enucleation fractions. **(G)** Volume measurements (left) from confocal image stacks of cytoplasmic and nuclear dyes in living REF52 intact cells (n = 55) and cytoplasts (n = 80). Calculated (calc.) cytosol was derived from pairwise subtraction of the empirically derived cytoplasmic volume from the nuclear volume for intact cells. Representative images are shown (right). Bar, 10 µm. **(H)** Cell spreading rates of REF52 intact cells and cytoplasts shown as area ± 95% CI over time. Intact + DMEM are untreated intact cells. Intact + FIC-CB are intact cells incubated in cytochalasin-containing Ficoll for 3 h without centrifugation. Treatments containing Ficoll and cytochalasin were washed before the experiment. Dotted vertical lines denote time at half-maximum rate of spreading for all treatments. Intact cells, n = 202; intact + FIC-CB, n = 127; cytoplasts, n = 194. Data in F, G, and H are from at least three experiments. One-way ANOVA with Tukey's post-hoc test was performed for F, and a Student's t test was performed for H. ***, $P < 0.001$; **, $P < 0.01$; *, $P < 0.05$. This figure is related to Fig. 1.

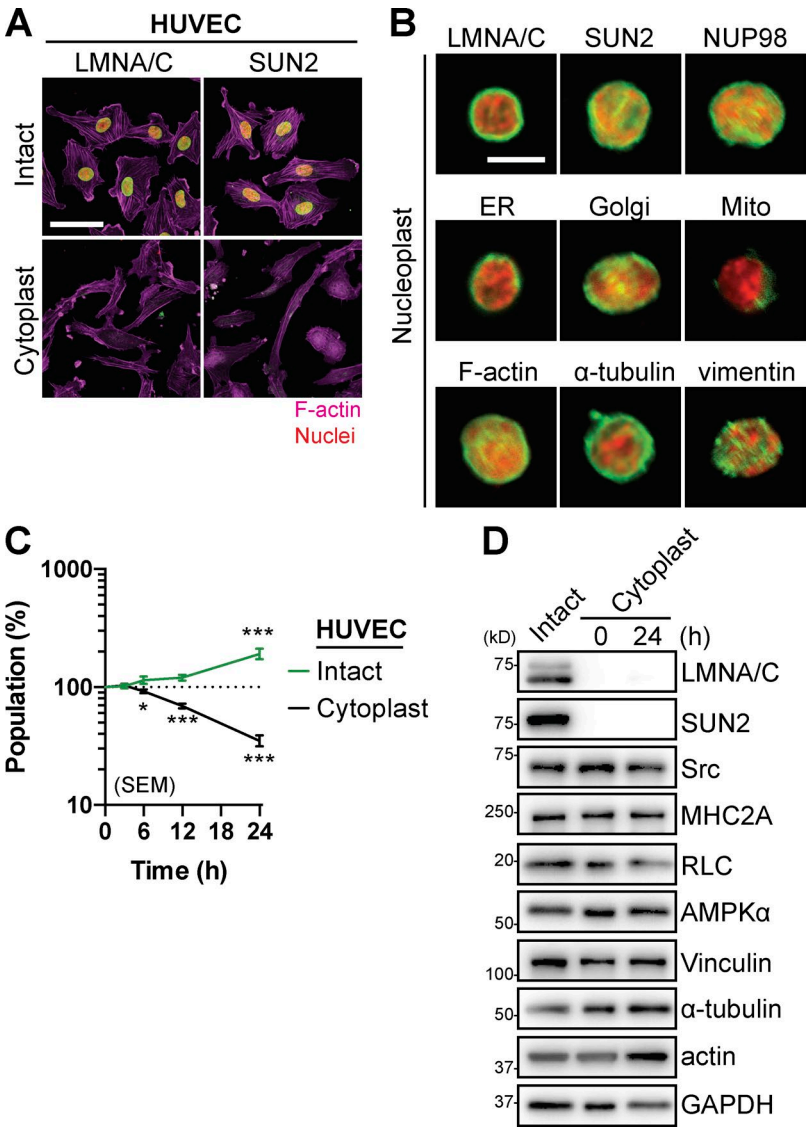

Figure S2. **Continued characterization of cytoplasts. (A)** Immunofluorescent staining of HUVEC cells for nuclear proteins. Bar, 50 µm. **(B)** Immunofluorescent staining of nucleoplasts. Nuclear stain is red. Bar, 10 µm. **(C)** Cell population as percent of starting population over time for HUVECs shown as mean ± SEM (n = 3 experiments). Student's t test performed between successive time points for either intact cells or cytoplasts. ***, $P < 0.001$; **, $P < 0.01$; *, $P < 0.05$. **(D)** Western blots of various cytoskeletal regulators from REF52 cytoplasts at 0 and 24 h after enucleation. RLC, myosin regulatory light chain. Cytoplasts were plated on FN until lysis at the 24-h time point. This figure is related to Fig. 1.

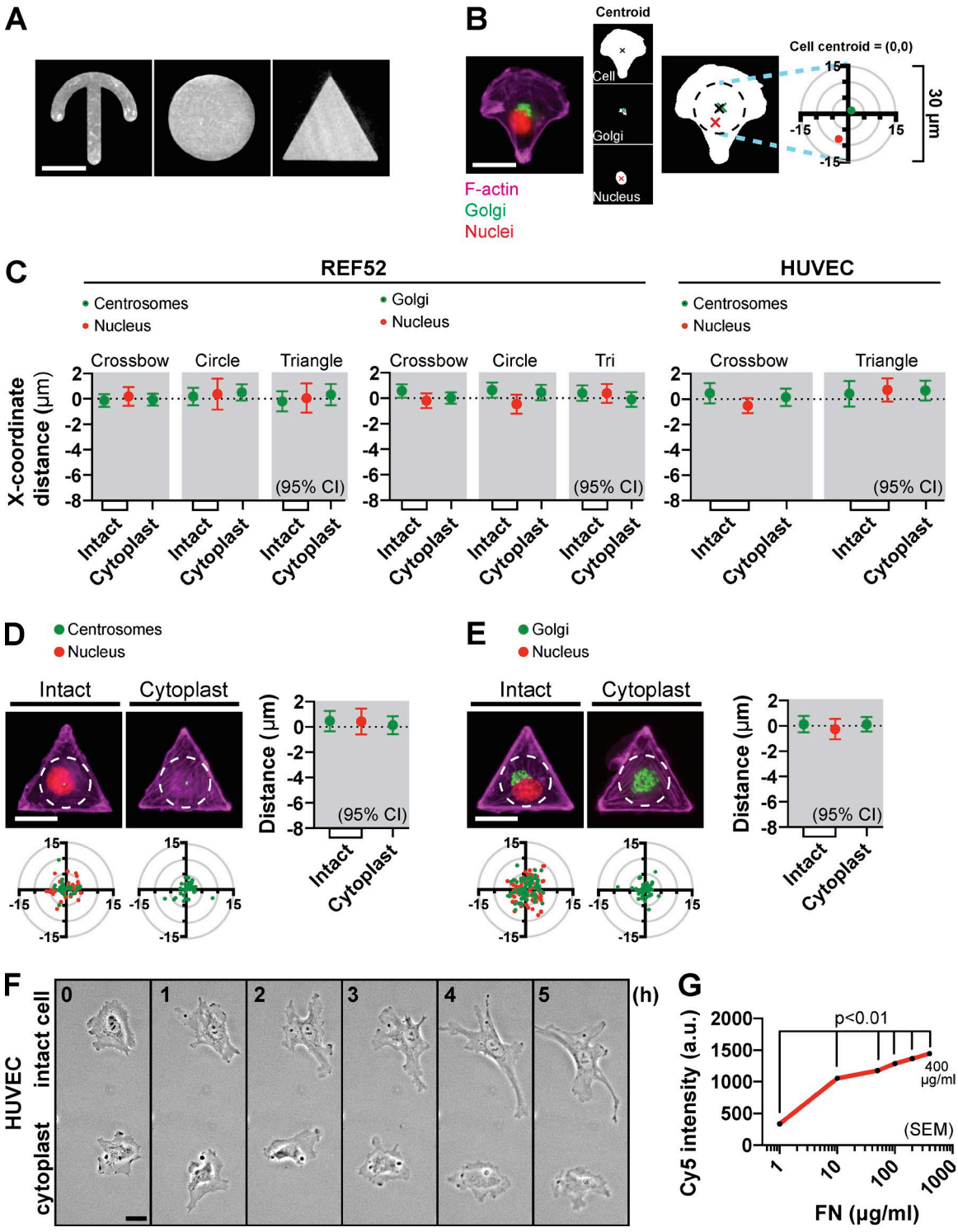

Figure S3. **Proper centrosome and Golgi positioning occurs in the absence of the nucleus. (A)** Patterns used for polarity work. Cy5-conjugated FN is shown in gray. **(B)** Image analysis and quantification approach used for pattern work. Raw three-channel image of an intact cell on a crossbow pattern. The centroid of each channel is calculated and normalized to the centroid of the cell (based on the F-actin channel). Organelle x,y-coordinate values are plotted on graph relative to cell centroid (shown as x,y = 0). **(C)** Mean x-coordinate values ± 95% CI for centrosomes (left) and the Golgi (middle) from REF52 intact cells and cytoplasts, and centrosomes (right) from HUVEC intact cells and cytoplasts, on different patterns. **(D)** Images (top left) and plots (bottom left) showing localization of centrosomes from REF52 cells on triangle patterns. Graph (right) showing mean distance ± 95% CI of centrosomes on triangle patterns. Intact cells, $n = 31$; cytoplasts, $n = 35$. **(E)** Images (top left) and plots (bottom left) showing localization of the Golgi from REF52 cells on triangle patterns. Graph (right) showing mean distance ± 95% CI of the Golgi on triangle patterns. Intact cells, $n = 78$; cytoplasts, $n = 50$. **(F)** Stills at 1-h intervals of HUVEC intact cell and cytoplast migrating. **(G)** Adsorbed Cy5-FN measured on glass with addition of various Cy5-FN concentrations ($n = 2$ experiments). A Student's *t* test performed between successive FN concentrations. Data in C–E are from at least three experiments. ***, $P < 0.001$; **, $P < 0.01$; *, $P < 0.05$. Bars, 25 µm. This figure is related to Fig. 2.

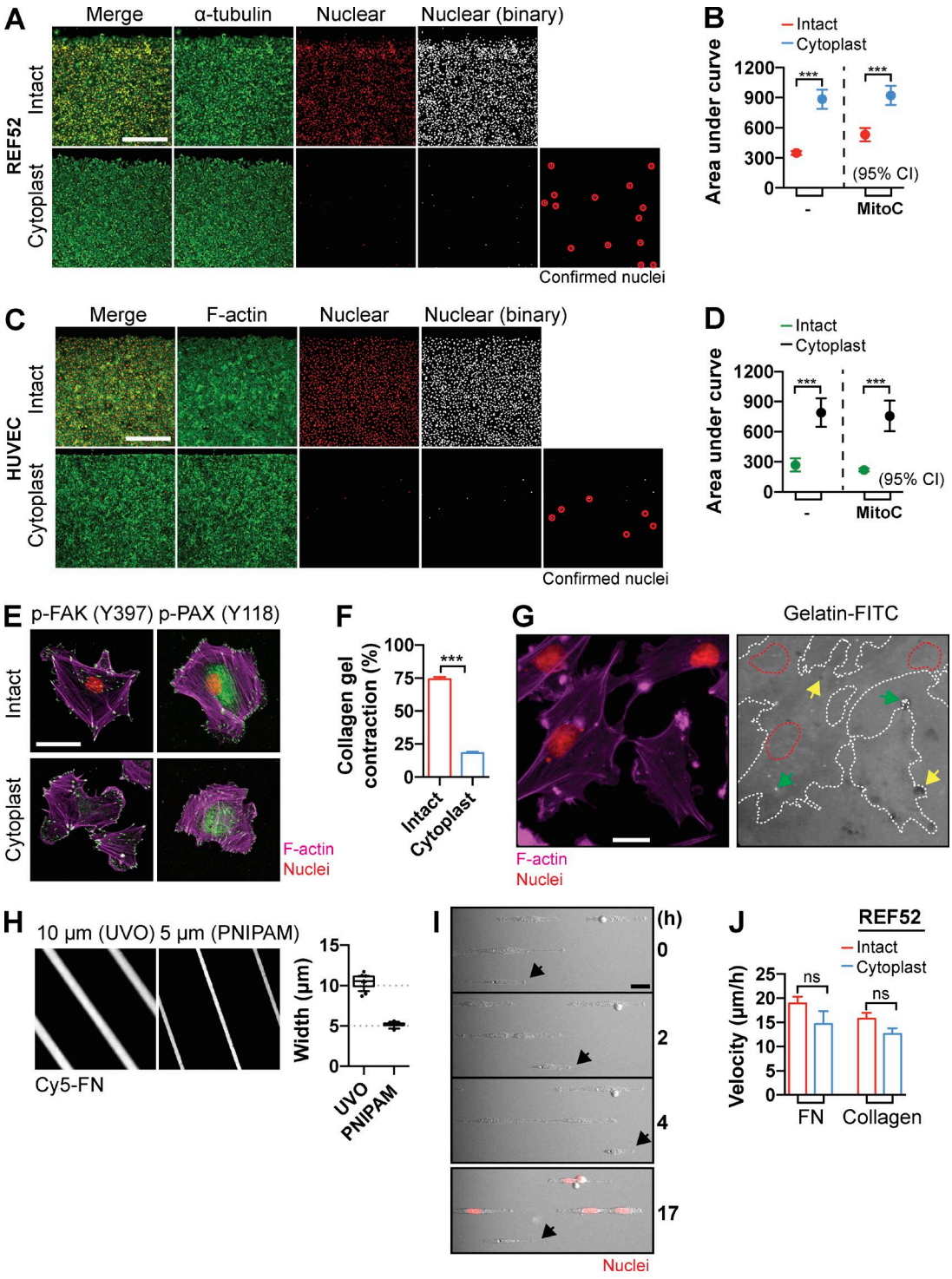

Figure S4. **1D and 2D cell migration occur in the absence of the nucleus. (A)** Wide-field images of REF52 cells behind the scratch margin that were stained for α-tubulin (green) and nuclei (red). Nuclear channel was converted to binary and nuclei were visually confirmed in the cytoplast population and outlined (red circles). Bar, 500 µm. **(B)** Mean area under the curve ± 95%CI for REF52 intact cells and cytoplasts from scratch assays shown in Fig. 4 (A and B). **(C)** Wide-field images of HUVECs behind the scratch margin that were stained for F-actin (green) and nuclei (red). Nuclear channel was converted to binary and nuclei were visually confirmed in the cytoplast population and outlined (red circles). Bar, 500 µm. **(D)** Mean area under the curve ± 95% CI for HUVEC intact cells and cytoplasts from scratch assays shown in Fig. 4 (E and F). **(E)** Immunofluorescent staining of REF52 cells on collagen-coated glass. Bar, 50 µm. **(F)** Mean percent collagen gel contraction ± SEM after 24 h. **(G)** Fluorescent images of REF52 intact cells and cytoplast on FITC-conjugated gelatin showing matrix degradation (yellow arrows) and matrix remodeling (green arrows). White dashed lines show cell outlines, and red dashed lines show nuclei. Bar, 20 µm. **(H)** Images (left) of 10-µm and 5-µm lines. Cy5-conjugated FN is shown in gray. Graph (right) showing measured line widths. Box plots show 10th to 90th percentile. UVO and PNIPAM refer to different methods used for line generation. **(I)** Stills of intact cells and cytoplasts on 5-µm lines. Arrows show cytoplasts. Bar, 10 µm. **(J)** Migration velocities (mean ± SEM) on 10-µm lines coated in 50 µg/ml FN (intact cells, $n = 36$; cytoplasts, $n = 34$) or 100 µg/ml collagen (intact cells, $n = 23$; cytoplasts, $n = 22$). A Student's t test was performed for B, D, F, and J. ***, $P < 0.001$; **, $P < 0.01$; *, $P < 0.05$. MitoC, mitomycin C. This figure is related to Figs. 4 and 5.

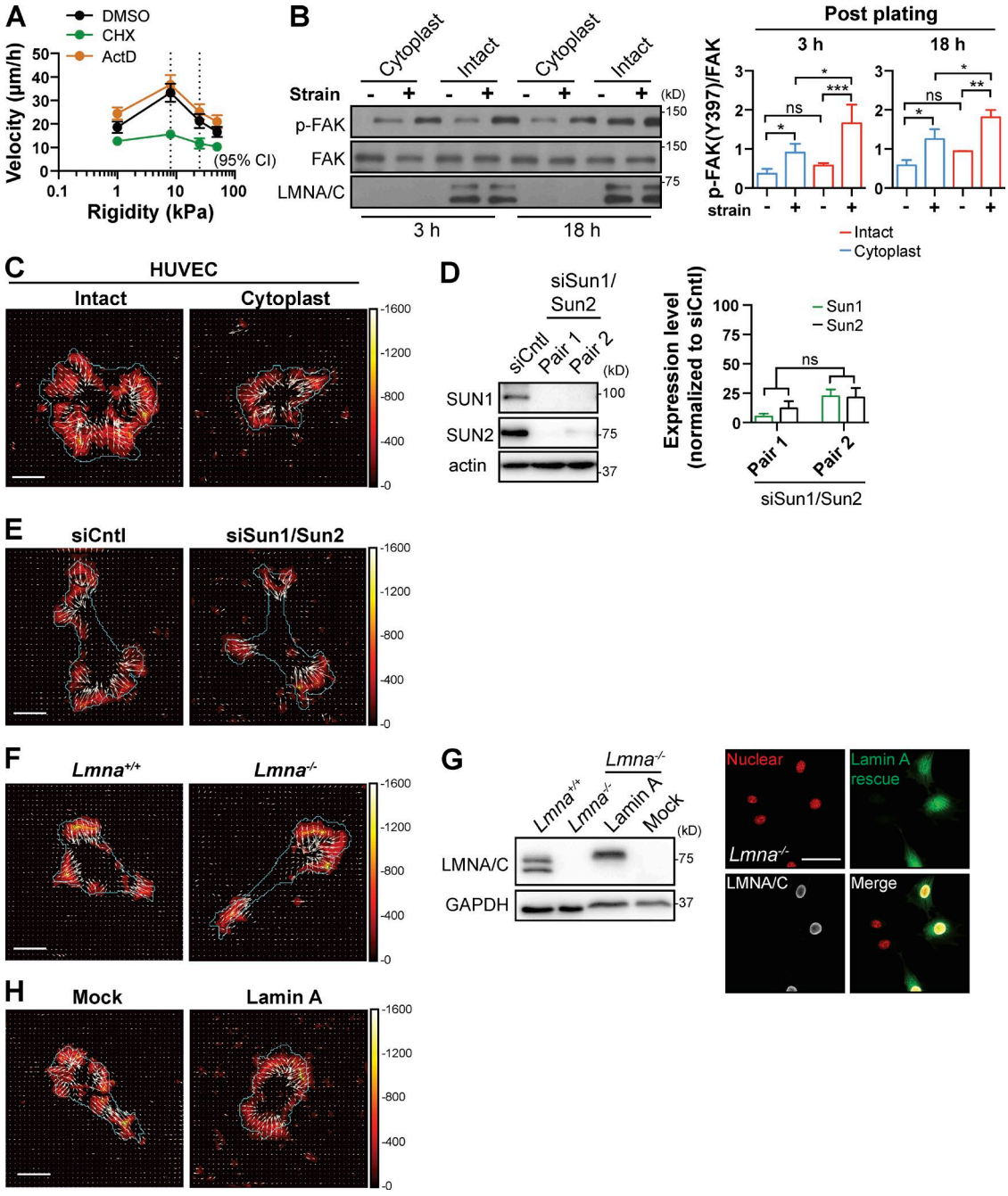

Figure S5. **The nucleus regulates cell contractility and the sensitivity of the cell to mechanical cues. (A)** Cell velocity ± 95% CI on compliant substrata for REF52 cells in the presence of DMSO ($n \geq 78$/stiffness), cycloheximide (CHX; $n \geq 46$/stiffness), or actinomycin D (ActD; $n \geq 71$/stiffness). **(B)** Western blot (left) of REF52 intact cells and cytoplasts from biaxial cyclic strain experiments. Graph (right) showing quantification (mean ± SEM) of blots from three experiments. **(C)** Representative images of HUVEC traction stresses. **(D)** Western blot (left) showing knockdown efficiency for siSun1/Sun2. Graph (right) showing quantification (mean ± SEM) of blots from three experiments. **(E)** Representative images of REF52 cells treated with siCntl or siSun1/Sun2 showing traction stresses. **(F)** Representative images of $Lmna^{+/+}$ and $Lmna^{-/-}$ cells showing traction stresses. **(G)** Western blot (top) of Lmna cell lines. Fluorescence images (bottom) of $Lmna^{-/-}$ cells mock or lamin A rescued. Bar, 50 µm. **(H)** Representative images of $Lmna^{-/-}$ cells mock or lamin A rescued. In C, E, F, and H, force vectors (white arrows), cell outlines (cyan), and scale showing traction stress magnitude (Pa), are shown. Bars: 20 µm (C, E, F, and H). One-way ANOVA with Newman–Keuls post-hoc test was performed for B. ***, $P < 0.001$; **, $P < 0.01$; *, $P < 0.05$. This figure is related to Figs. 6 and 7.

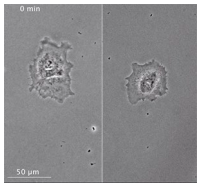

Video 1. **REF52 cytoplasts exhibit anterior–posterior polarity, dynamic lamellipodial extension, and rear retraction during migration.** Intact cell (left) and cytoplast (right) randomly migrating on FN. Images were acquired every 10 min for 24 h using a 20× magnification on a Nikon Biostation IM microscope.

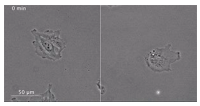

Video 2. **HUVEC cytoplasts exhibit anterior–posterior polarity, dynamic lamellipodial extension, and rear retraction during migration.** Intact cell (left) and cytoplast (right) randomly migrating on FN. Images were acquired every 10 min for 10 h using a 20× magnification on a Nikon Biostation IM microscope.

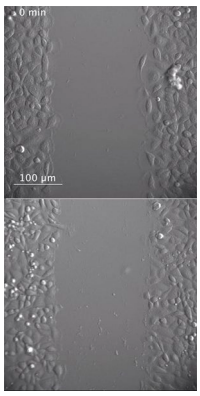

Video 3. **Scratch-wound closure occurs independent of the nucleus in REF52 cells.** A scratch assay showing intact cells (top) and cytoplasts (bottom) from mitomycin C–pretreated cells. Immediately after creating a scratch, intact cells and cytoplasts polarize and migrate into the cleft. Images were acquired every 10 min for 16 h using a 20× objective under 0.5× magnification on an Olympus VivaView FL microscope.

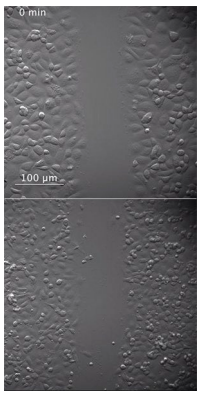

Video 4. **Scratch-wound closure occurs independent of the nucleus in HUVECs.** A scratch assay showing intact cells (top) and cytoplasts (bottom) from mitomycin C–pretreated cells. Immediately after creating a scratch, intact cells and cytoplasts polarize and migrate into the cleft. A narrower scratch was used for these experiments to limit closure effects caused by decreased survival of HUVEC cytoplasts. Images were acquired every 10 min for 16 h using a 20× objective under 0.5× magnification on an Olympus VivaView FL microscope.

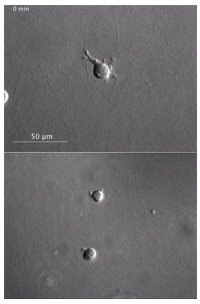

Video 5. **3D migration in collagen matrices is dependent on the nucleus in REF52 cells.** An intact cell (top) and cytoplasts (bottom) migrating in an LR 3D collagen matrix. Intact cells and cytoplasts extend protrusions that engage with nearby collagen fibers, however, cytoplasts are nonmigratory in 3D. Images were acquired every 10 min for 12 h using a 40× objective on an Olympus VivaView FL microscope.

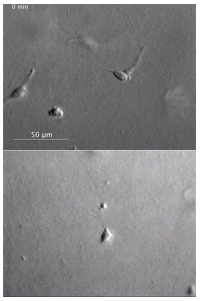

Video 6. **3D migration in collagen matrices is dependent on the nucleus in HUVECs.** An intact cell (top) and cytoplasts (bottom) migrating in an LR 3D collagen matrix. Intact cells and cytoplasts extend protrusions that engage with nearby collagen fibers, however, cytoplasts are nonmigratory in 3D. Images were acquired every 10 min for 10 h using a 40× objective on an Olympus VivaView FL microscope.

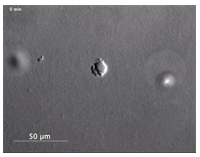

Video 7. **Cytoplasts can engage and displace collagen fibers.** A REF52 cytoplast migrating in an LR 3D collagen matrix. The cytoplast displaces collagen fibers but is unable to migrate. Images were acquired every 10 min for 12 h using a 40× objective on an Olympus VivaView FL microscope.

Video 8. **1D migration is not dependent on the nucleus. REF52 intact cells and a single cytoplast (at bottom of frame) migrating on 5-µm-wide 1D lines.** In this video, images were acquired every 10 min for up to 5.5 h using a 20× objective under 0.5× magnification on an Olympus VivaView FL microscope.